Coherence effects in triplet-exciton transport via time-dependent delayed fluorescence

V. M. Kenkre,* V. Ern, and A. Fort
Laboratoire de Spectroscopie et d'Optique du Corps Solide, Laboratoire (No. 232) associé au Centre National de la Recherche Scientifique, Université Louis Pasteur, 5 rue de l'Université, F-67000 Strasbourg, France
(Received 9 March 1983)

We develop a theory for experiments on triplet-exciton transport involving the measurement of the evolution of spatially periodic inhomogeneities in the exciton population with the help of observations of delayed fluorescence. The theory is based on generalized master equations and therefore allows the study of explicit effects of transport coherence for arbitrary degree of coherence. A specific application to one-dimensional crystals is also given with detailed prescriptions to extract relevant transport parameters from experiments.

I. INTRODUCTION

This paper combines an established, direct, experimental technique for transport measurements of triplet Frenkel excitons in molecular crystals with a relatively recent theoretical approach for the analysis of exciton transport. The experimental method is that of Ronchi rulings.[1-6] The theoretical formalism is that of generalized master equations.[7-12] The primary goal of the present analysis is the elucidation of the observable effects of transport coherence on Ronchi ruling signals.

A variety of experimental procedures[1-6,13-22] have been employed to study triplet-exciton motion in molecular crystals. The method of Ronchi rulings possesses the advantages of directness and the relative facility it provides one to subtract contributions from spurious effects. A number of experiments based on this method have been carried out and the anisotropy of the triplet-exciton diffusion tensor has been determined in several crystals.[2,4] However, the theoretical analysis used in conjunction with these experiments has been based, up to now, on the simple diffusion equation. Clearly, transport subtleties such as coherence, which have long been suspected[13-22] to exist in exciton motion, are not amenable to analysis in terms of the diffusion equation since the latter implies, from the very start, completely incoherent motion. In recent years two transport techniques have been developed precisely with the intention of describing such transport subleties: that of generalized master equations[7-12] and that of stochastic Liouville equations.[23-25] The relationships between the two techniques have been investigated in considerable detail.[26] The method of generalized master equations is particularly appropriate[9] to the investigation of direct migration experiments such as those involving Ronchi rulings. We have therefore begun a thorough analysis of the latter based on generalized master equations.

The basic idea behind Ronchi ruling experiments can be described as follows. If one shines light on a crystal and thereby creates triplet excitons in a region small enough so that a substantial fraction of the excitons can move out of that region within their lifetime, the delayed fluorescence signal arising from the mutual annihilation of the excitons decays in time as a result not only of the finiteness of the lifetime but also of the motion. This is so because the faster the motion, the more is the depletion of the population from the initially illuminated region and the signal is, in essence, proportional to the square of the population. To make the signal strong enough to become observable, light is made to shine not on a single small region but through a periodic linear array of alternating opaque and transparent strips (the Ronchi ruling) placed under the crystal, and the delayed fluorescence signal is collected from the *entire* crystal.

The emission is observed in a time-dependent fashion both during the buildup part when the light source is on at a constant nonzero intensity, and during the decay part when the source is shut off. For experimental details the reader is referred to Ref. 1. While it is possible, in principle, to study the steady-state (rather than time-dependent) signal in such a setup, there are a number of experimental pitfalls in the interpretation of such observations which can easily lead to an overestimation of the diffusion constant. This problem is avoided in time-dependent measurements because it is possible to subtract the signal one would have if exciton motion were absent.[1] This is an essential feature of this kind of experiment which helps in the practical elimination of spurious effects. While it is evidently impossible to cause the excitons to refrain from moving, it is possible to make observations in the absence of rulings. One still has a delayed fluorescence signal which contains several of the same spurious contributions that are present in the signal with rulings but does not contain the contribution from exciton motion. The difference of the two normalized signals, which we call $\Delta\Phi(t)$ in what follows, is thus directly sensitive to exciton motion.

The special feature of the theoretical technique of generalized master equations (GME) is that it is capable of providing a unified analysis of coherent and incoherent motion. It is not necessary to borrow band concepts in one limit, diffusion or hopping concepts in the other limit and move from one transport equation to another as the system conditions change. The memory functions in the GME, and particularly the essential time dependence of those memory functions, allow such a unification. It is thus possible to provide a single expression for the experimental signal valid for arbitrary degrees of coherence and to use it to interpret the observations. Furthermore, it is possible on the one hand to obtain the GME memory functions from spectral observations or detailed model calculations and thus have that information reflected in the interpretation of the particular experiment. On the other

hand, it is also possible to use GME's corresponding to simple intuitive pictures such as that involving the mean free path of the exciton. The signal predicted by the GME can thus be studied not only in the extreme diffusive limit when the mean free path is smaller than a lattice constant (the intersite distance) and in the extreme coherent limit when the mean free path is infinite (total absence of scattering) but as we shall show below, it can be analyzed explicitly for the entire intermediate range.

The combination of the GME approach and the Ronchi ruling technique will be seen to have several interesting consequences. It is clear that the effect of coherence will depend on the magnitude of the ratio of the mean free path to the lattice constant, or, what is essentially the same, the ratio of the exciton bandwidth to the scattering rate. Systematic experimental variation of the bandwidth is not feasible in general. It will be seen, however, that, in the experimental approach under discussion, one deals instead with a quantity which is the bandwidth reduced by the ratio of the lattice constant to the ruling period.[27] Systematic variation of the ruling period is certainly possible. It is thus that a systematic study of exciton coherence is possible, at least in principle, via the GME analysis of Ronchi ruling experiments. Of the four characteristic lengths that are present in the system, the lattice constant, the mean free path, the diffusion length, and the period of the Ronchi rulings, only the last two have appeared in previous analyses of the experiment. The present analysis will show that if the ruling period, the experimentally controllable quantity, is manipulated as to be of the order of the mean free path, new observable features visible in the time dependence of the signal appear. A practical discussion of how the degree of coherence may be determined from those features will be found in Sec. IV below. The rest of the paper is laid out as follows. The theoretical analysis leading to general expressions for the experimental signals is displayed in Secs. II and III. Particular cases and plots are given in Sec. IV. They include the case of motion with arbitrary degree of coherence as well as the limits of pure coherence and of complete incoherence. A discussion of the assumptions underlying the theory forms Sec. V, and concluding remarks appear in Sec. VI.

II. EXACT EXPRESSIONS FOR EXCITON PROBABILITIES IN THE RONCHI GEOMETRY

The starting point of our analysis is the augmented generalized master equation (GME) obeyed by the probabilities $P_m(t)$ of occupation by the exciton of the site m in the crystal at time t:

$$\frac{dP_m(t)}{dt}=\int_0^t dt' \sum_n [W_{mn}(t-t')P_n(t')-W_{nm}(t-t')P_m(t')]-\frac{P_m(t)}{\tau}+\mathcal{I}_m(t)-\gamma' P_m^2(t) . \tag{2.1}$$

We use the term "augmented" here to refer to the presence of the last three terms in (2.1). These additional three terms represent, respectively, exciton decay with lifetime τ, exciton creation through the illumination source $\mathcal{I}_m(t)$, and mutual annihilation of excitons with an annihilation constant which equals γ except for a proportionality factor of a unit cell volume.[9] The $W_{mn}(t)$'s in the standard GME are memory functions capable of describing exciton motion with arbitrary degree of coherence. In the limit of complete incoherence they are delta functions in time and are proportional to the transition rates for the exciton to move from site n to site m.

Various details about the validity of the GME, its capability to unify coherent and incoherent motion, and expressions, microscopic and otherwise, that can be obtained for its $W_{mn}(t)$'s have been given elsewhere.[9] Suffice it to state that essentially all limiting cases of interest can be obtained from (2.1) by varying the W's appropriately.

Concerning the three additional terms in (2.1) the following statements are appropriate: (a) τ is the total lifetime including both the radiative and radiationless contributions. (b) Although some questions exist[9,11] about the validity of the traditional form for the bilinear annihilation term $\gamma' P_m^2(t)$ it can be shown (see Sec. V) that, for the present analysis of Ronchi grating signals, its use is indeed valid. (c) The specific form for the source term $\mathcal{I}_m(t)$ used below is representative of the particular (spatially periodic) geometry and of the time dependence of the excitation.

It is well known that the solution of (2.1) *without* the three additional terms can be written in terms of initial conditions as

$$P_m(t)=\sum_n \psi_{m-n}(t)P_n(0) , \tag{2.2}$$

where the ψ's are the propagators. Specifically, $\psi_{mn}(t)$ is the solution of (2.1) (without the three additional terms), i.e., the probability of occupation of site m at time t, for the special initial condition that site n was occupied at time 0. Translational invariance (periodicity) of the crystal allows one to write ψ_{mn} as the single-indexed quantity ψ_{m-n}.

One now considers experimental conditions involving small enough illumination intensities so that the last term in (2.1) can be neglected,[1] and then uses the solutions thus obtained to get from that term the experimentally observable signal, viz., the delayed fluorescence. This procedure is being followed to be faithful to the experiment[1] and not out of an inability to solve (2.1). The transport equation in the presence of the annihilation terms can indeed be solved exactly at least for medium intensities of illumination.[9,11]

The solution of (2.1) without the last term is given generally in the Laplace domain as

$$\tilde{P}_m(\epsilon)=\sum_n \tilde{\psi}_{m-n}(\epsilon')P_n(0)+\sum_n \tilde{\psi}_{m-n}(\epsilon')\tilde{\mathcal{I}}_n(\epsilon) . \tag{2.3}$$

Here, and henceforth in the paper, tildes denote Laplace transforms and ϵ is the Laplace variable. The ϵ' appearing in $\tilde{\psi}$ in (2.3) equals $\epsilon+1/\tau$.

As mentioned in Sec. I, the Ronchi grating experiments[1]

consist of two parts, one in which the delayed fluorescence builds up to its saturation value under the action of a constant (in time) illumination source, and the other in which the source is shut off and the delayed fluorescence decays from the saturation value. For the buildup part there are no excitons initially in the system, $P_n(0)=0$ and (2.3) gives

$$\epsilon\tilde{P}_m(\epsilon)=\sum_n \tilde{\psi}_{m-n}(\epsilon')g_n i_0 , \tag{2.4}$$

where one takes the illumination source to be

$$\mathscr{I}_n(t)=i_0 g_n \Theta(t) \tag{2.5}$$

with i_0 as the intensity of illumination multiplied by the appropriate $S_0\rightarrow T_1$ absorption coefficient, g_m as the function characteristic of the ruling geometry and $\Theta(t)$ as the Heaviside unit step function. Introducing discrete Fourier transforms such as P^k, ψ^k, g^k through relations such as

$$P^k=\sum_m P_m e^{ikm} , \tag{2.6}$$

where the summation is over all the N sites of the crystal (assumed, as usual, to obey periodic boundary conditions or to be infinite in extent), one rewrites (2.4) as

$$\epsilon\tilde{P}^k(\epsilon)=\tilde{\psi}^k(\epsilon')g^k i_0 . \tag{2.7}$$

The ruling geometry imposes the relation[6]

$$g^k=\frac{1}{2}\left[\delta_{k,0}+\sum_{l=1}^{\infty} S_l(\delta_{k,\eta_l}+\delta_{k,-\eta_l})\right] , \tag{2.8}$$

$$S_l=-\frac{2}{\pi(2l-1)}\sin\left[\frac{\pi(2l-1)}{2}\right] , \tag{2.9}$$

where the opaque and transparent strips alternate with the grating period x_0. Needless to say, (2.8) is simply the Fourier transform of a square wave.[28] We have used here the definition of a dimensionless wavevector η_l through

$$\eta_l=2\pi\frac{a}{x_0}(2l-1) , \tag{2.10}$$

where a is the lattice constant. The substitution of (2.8) in (2.7) yields, with $q_0=N(i_0\tau)^{-1}$,

$$(q_0\tau)\epsilon\tilde{P}_m(\epsilon)=\frac{1}{2}\left[\frac{1}{\epsilon+\frac{1}{\tau}}\right]+\sum_{l=1}^{\infty} S_l\cos(\eta_l m)\left[\tilde{\psi}^{\eta_l}\left[\epsilon+\frac{1}{\tau}\right]\right] \tag{2.11}$$

as the solution, in the Laplace domain, of the exciton occupation probabilities P_m for the buildup part of the signal. Equation (2.11) may be used in two ways. By inverting it one obtains the time domain solution

$$q_0P_m(t)=\tfrac{1}{2}(1-e^{-t/\tau})+\sum_{l=1}^{\infty} S_l\cos(\eta_l m)\left[\frac{1}{\tau}\int_0^t dt' e^{-t'/\tau}\psi^{\eta_l}(t')\right] \tag{2.12}$$

whereas by taking the limit of (2.11) as $\epsilon\rightarrow\infty$ [or the limit of (2.12) as $t\rightarrow\infty$] one obtains the steady-state saturation value

$$q_0P_m(\infty)=\tfrac{1}{2}+\sum_{l=1}^{\infty} S_l\cos(\eta_l m)\left[\frac{1}{\tau}\tilde{\psi}^{\eta_l}\left[\frac{1}{\tau}\right]\right] . \tag{2.13}$$

For the decay part of the experiment one returns to (2.3), substitutes the saturation values $P_n(\infty)$ given by (2.13) as the initial values $P_n(0)$ in (2.3), and, since no source term $\mathscr{I}$ exists, obtains

$$q_0\tilde{P}_m(\epsilon)=\frac{1}{2}\left[\frac{1}{\epsilon+\frac{1}{\tau}}\right]+\sum_{l=1}^{\infty} S_l\cos(\eta_l m)\left[\frac{1}{\tau}\tilde{\psi}^{\eta_l}\left[\frac{1}{\tau}\right]\right]\tilde{\psi}^{\eta_l}\left[\epsilon+\frac{1}{\tau}\right] \tag{2.14}$$

for the decay probabilities. A Laplace inversion gives

$$q_0P_m(t)=\tfrac{1}{2}e^{-t/\tau}+\sum_{l=1}^{\infty} S_l\cos(\eta_l m)\left[\frac{1}{\tau}\tilde{\psi}^{\eta_l}\left[\frac{1}{\tau}\right]\right]e^{-t/\tau}\psi^{\eta_l}(t) . \tag{2.15}$$

Equations (2.13) for the saturation value, and (2.12) and (2.15) for the buildup and decay cases, respectively, contain the explicit expressions we have obtained for exciton probabilities. It is to be stressed that they are valid whether or not a diffusion equation or a master equation or a pure Schrödinger equation is valid. Whatever the nature of the motion is, the appropriate ψ^{η_l} (Fourier transform of the propagator) may be used in the expressions. It will be seen in Sec. IV how the nature of the motion decides the form of ψ^{η_l} and thence the time dependence of the signal. It is worth noticing the similarities and differences in the buildup and decay cases. The second terms of both are identical except that $e^{-t/\tau}\psi^{\eta_l}(t)$ appears in the decay case while its integral up to time t (normalized by τ) appears in the buildup case. Similarly, the first terms are related in that $e^{-t/\tau}$ appears in the decay case but its integral (normalized by τ), i.e., $1-e^{-t/\tau}$ appears in the buildup case.

III. EXPLICIT SIGNALS FOR THE DELAYED FLUORESCENCE

Since the delayed fluorescence signal is proportional to $\sum_m P_m^2(t)$, one squares and sums (2.13), (2.12), and (2.15) over the entire crystal to obtain

$$\sum_m P_m^2(\infty)=c\left[1+\sum_{l=1}^{\infty} A_l\right] , \tag{3.1}$$

$$\sum_m P_m^2(t)=c\left[(1-e^{-t/\tau})^2+\sum_{l=1}^{\infty}A_l\left[\frac{\int_0^t dt' e^{-t'/\tau}\psi^{\eta_l}(t')}{\int_0^\infty dt' e^{-t'/\tau}\psi^{\eta_l(t')}}\right]^2\right], \tag{3.2}$$

$$\sum_m P_m^2(t)=c\left[e^{-2t/\tau}+\sum_{l=1}^{\infty}A_l[e^{-t/\tau}\psi^{\eta_l}(t)]^2\right], \tag{3.3}$$

where the constant c is proportional to $(i_0\tau)^2$. Equation (3.2) refers to the buildup part, (3.3) to the decay part, and (3.1) to the saturation value. The coefficients A_l are defined by

$$A_l=\frac{8}{\pi^2(2l-1)^2}\left[\frac{1}{\tau}\tilde{\psi}^{\eta_l}\left[\frac{1}{\tau}\right]\right]^2. \tag{3.4}$$

The symbol $\Phi(t)$ will be used to denote $\sum_m P_m^2(t)/\sum_m P_m^2(\infty)$, i.e., the signal normalized to the saturation value. The superscripts b and d will be used to represent buildup and decay, respectively. The normalized signals are then

$$\Phi^b(t)=\left[1+\sum_{l=1}^{\infty}A_l\right]^{-1}\left[(1-e^{-t/\tau})^2+\sum_{l=1}^{\infty}\frac{8}{\pi^2(2l-1)^2}\left[\frac{1}{\tau}\int_0^t dt' e^{-t'/\tau}\psi^{\eta_l}(t')\right]^2\right], \tag{3.5}$$

$$\Phi^d(t)=\left[1+\sum_{l=1}^{\infty}A_l\right]^{-1}\left[1+\sum_{l=1}^{\infty}A_l[\psi^{\eta_l}(t)]^2\right]e^{-2t/\tau}. \tag{3.6}$$

We have explained in Sec. I how careful experimentation requires that attention be focused on the *difference* between these signals and their values in the absence of motion, or equivalently in the absence of rulings ($x_0\to\infty$). These are given merely by subtracting $e^{-2t/\tau}$ and $(1-e^{-t/\tau})^2$ from the right-hand sides of (3.6) and (3.5), respectively. One gets

$$\Delta\Phi^b(t)=(1-e^{-t/\tau})^2E^b(t), \tag{3.7}$$

$$\Delta\Phi^d(t)=e^{-2t/\tau}E^d(t). \tag{3.8}$$

The functions $(1-e^{-t/\tau})^2$ and $e^{-2t/\tau}$ appearing in the right-hand sides of (3.7) and (3.8) are the respective values of the buildup signal Φ^b and the decay signal Φ^d *in the absence of rulings.* The functions $E^b(t)$ and $E^d(t)$ which multiply them in the presence of rulings contain information about exciton motion and are given by

$$E^b(t)=\left[1+\sum_{l=1}^{\infty}A_l\right]^{-1}\left\{\sum_{l=1}^{\infty}A_l\left[\left[\frac{\int_0^t dt' e^{-t'/\tau}\psi^{\eta_l}(t')}{(1-e^{-t/\tau})\tilde{\psi}^{\eta_l}(1/\tau)}\right]^2-1\right]\right\}. \tag{3.9}$$

$$E^d(t)=\left[1+\sum_{l=1}^{\infty}A_l\right]^{-1}\left[\sum_{l=1}^{\infty}A_l\{[\psi^{\eta_l}(t)]^2-1\}\right]. \tag{3.10}$$

We have written (3.9) in a slightly complex fashion to emphasize its formal relation to (3.10). Needless to say it can be written more simply for computational purposes.

IV. PARTICULAR CASES AND APPLICATION TO POSSIBLE EXPERIMENTS

We now study particular cases of the general expressions (3.7)—(3.10) for the Ronchi ruling signals by simply substituting the appropriate propagators ψ^{η_l} in them. Consider for simplicity only one-dimensional crystals and basic nearest-neighbor interactions. If the motion is completely incoherent, the appropriate transport equation is

$$\frac{dP_m(t)}{dt}=F(P_{m+1}+P_{m-1}-2P_m) \tag{4.1}$$

wherein F is the nearest-neighbor transfer rate related simply to the diffusion constant D through

$$D=Fa^2 \tag{4.2}$$

with a as the lattice constant. If, on the other hand, the motion is completely coherent, i.e., if an initially populated band state is never scattered, the appropriate transport equation in real space is the Schrödinger equation

$$\frac{dC_m}{dt}=-iV(C_{m+1}+C_{m-1}) \tag{4.3}$$

obeyed by the *amplitude* $C_m(t)$, where V is the nearest-neighbor transfer matrix element which is proportional to the exciton bandwidth. The corresponding equation obeyed by the probability $P_m(t)$ is the GME with the memory[9,12]

$$W_{mn}(t)=\frac{1}{t}\frac{d}{dt}J_{m-n}^2(2Vt)\equiv W_{mn}^{\mathrm{coh}}(t). \tag{4.4}$$

The coherent case represented by (4.3) or (4.4) and the incoherent case represented by (4.1) or by

$$W_{mn}(t)=F(\delta_{m,n+1}+\delta_{m,n-1})\delta(t) \tag{4.5}$$

are both extremes of a general situation represented by the GME with the memories

$$W_{mn}(t)=W_{mn}^{\mathrm{coh}}(t)e^{-\alpha t}\ . \tag{4.6}$$

The $W_{mn}^{\mathrm{coh}}(t)$ is the coherent memory of (4.4) and α is the rate of scattering. We refer the reader to Refs. 9 and 12 for further elaboration of these memories and Sec. V below for a further discussion of the physical meaning of (4.6).

The Fourier transforms $\psi^{\eta_l}(t)$ of the propagators $\psi_m(t)$ corresponding to these three cases are of interest to the present analysis. They have all been calculated elsewhere.[9] Thus the perfectly incoherent propagator corresponding to (4.1), (4.5) is

$$\psi_m(t)=e^{-2Ft}I_m(2Ft)\ , \tag{4.7}$$

where I_m is the mth modified Bessel function. This leads to

$$\psi^{\eta_l}(t)=e^{-4Ft\sin^2(\eta_l/2)}\ , \tag{4.8}$$

$$(1/\tau)\tilde{\psi}^{\eta_l}(1/\tau)=[1+4F\tau\sin^2(\eta_l/2)]^{-1}\ . \tag{4.9}$$

The perfectly coherent propagator corresponding to (4.3), (4.4) is

$$\psi_m(t)=J_m^2(2Vt)\ , \tag{4.10}$$

where J_m is the mth ordinary Bessel function. This leads to

$$\psi^{\eta_l}(t)=J_0(4Vt\sin(\eta_l/2))\ , \tag{4.11}$$

$$(1/\tau)\tilde{\psi}^{\eta_l}(1/\tau)=[1+16(V\tau)^2\sin^2(\eta_l/2)]^{-1/2}\ . \tag{4.12}$$

The intermediate coherence case has also been worked out completely.[9] A new, simple, and particularly convenient form for the intermediate propagator has been given recently.[29] It is

$$\psi_m(t)=J_m^2(2Vt)e^{-\alpha t}+\int_0^t du\,\alpha e^{-\alpha(t-u)}J_m^2[2V(t^2-u^2)^{1/2}]\ . \tag{4.13}$$

It leads to

$$\psi^{\eta_l}(t)=J_0(4Vt\sin(\eta_l/2))e^{-\alpha t}+\int_0^t du\,\alpha e^{-\alpha(t-u)}J_0((t^2-u^2)^{1/2}4V\sin(\eta_l/2))\ , \tag{4.14}$$

$$(1/\tau)\tilde{\psi}^{\eta_l}(1/\tau)=\{[(1+\alpha\tau)^2+16(V\tau)^2\sin^2(\eta_l/2)]^{1/2}-\alpha\tau\}^{-1}\ . \tag{4.15}$$

It is clear that Eqs. (4.13)–(4.15) reduce to the above given extreme cases in the respective limits. These limits are $\alpha\to 0$ (coherent) and $\alpha\to\infty, V\to\infty, 2V^2/\alpha=F$ (incoherent).

From (2.10) it is obvious that η_l is a very small quantity (relative to 1) since the lattice constant a is of the order of 5 or 10 Å whereas the ruling period x_0 is typically of the order of several microns (or larger) for all practical rulings. It follows then that the replacement

$$\sin(\eta_l/2)\simeq\eta_l/2 \tag{4.16}$$

is amply valid. While there is no need to make such a replacement in the above expressions (they may be used as given) we shall make it in the light of the applicable values and write

$$4F\sin^2(\eta_l/2)\simeq 4\pi^2F(a/x_0)^2(2l-1)^2\ , \tag{4.17}$$

$$8V^2\sin^2(\eta_l/2)\simeq 8\pi^2(Va/x_0)^2(2l-1)^2\ . \tag{4.18}$$

This replacement, which is nothing other than the continuum approximation, yields

$$\frac{1}{\tau}\tilde{\psi}^{\eta_l}\left[\frac{1}{\tau}\right]=\{[(1+\alpha\tau)^2+(4\pi V\tau a/x_0)^2(2l-1)^2]^{1/2}-\alpha\tau\}^{-1} \tag{4.19}$$

for the general case, the coherent and incoherent extremes being, respectively,

$$\frac{1}{\tau}\tilde{\psi}^{\eta_l}\left[\frac{1}{\tau}\right]=[1+(4\pi V\tau a/x_0)^2(2l-1)^2]^{-1/2}\ , \tag{4.20}$$

$$\frac{1}{\tau}\tilde{\psi}^{\eta_l}\left[\frac{1}{\tau}\right]=[1+(2\pi\sqrt{F\tau}a/x_0)^2(2l-1)^2]^{-1}\ . \tag{4.21}$$

For the subsequent discussion it is convenient to introduce a "transport length" l_T, defined as the average distance traveled by the exciton during its lifetime, whatever its degree of coherence. It is a generalization of the well-known diffusion length l_D to which it reduces under completely incoherent conditions. For the model of the present section l_T is given by

$$l_T=2a(V/\alpha)(\alpha\tau-1+e^{-\alpha\tau})^{1/2}\ . \tag{4.22}$$

Equation (4.22) is obtained by calculating for this model, the mean-square displacement[9] at $t=\tau$ and equating it to the square of l_T. Crucial to the physics of the experiments under discussion is the ratio l_T/x_0. While the underlying picture in the incoherent limit is that of an exciton moving across the ruling period as a random walker ($l_T/x_0=\sqrt{2}\sqrt{F\tau}a/x_0$), in the coherent limit the exciton is envisaged as moving without scattering and with a velocity $\sqrt{2}Va$ ($l_T/x_0=\sqrt{2}V\tau a/x_0$). Equations (4.20) and (4.21) may now be rewritten in terms of this ratio of the transport length to the ruling period. In the purely coherent limit, the delayed fluorescence signals (3.7) and (3.8) are given by

$$\Delta\Phi^b(t)=(1-e^{-t/\tau})^2(2S^{\mathrm{coh}})^{-1}\left\{\sum_{l=1}^{\infty}A_l\left[\left[\int_0^t dt' J_0(z_l t')\right]^2-1\right]\right\}\ , \tag{4.23}$$

$$\Delta\Phi^d(t)=e^{-2t/\tau}(2S^{\rm coh})^{-1}\left[\sum_{l=1}^{\infty}A_l[J_0^2(z_l t)-1]\right], \tag{4.24}$$

where $S^{\rm coh}=1-(2\sqrt{2}l_T/x_0)\tanh(x_0/4\sqrt{2}l_T)$, where $z_l=(2l-1)(2\pi\sqrt{2}l_T/x_0)(1/\tau)$, and A_l are given by (3.4) and (4.20).

In the completely incoherent limit, one recovers the results of Ref. 1:

$$\Delta\Phi^b(t)=(1-e^{-t/\tau})^2(2S^{\rm inc})^{-1}\left\{\sum_{l=1}^{\infty}A_l\left[\left[\int_0^t dt' e^{-y_l^2 t'}\right]^2-1\right]\right\}, \tag{4.25}$$

$$\Delta\Phi^d(t)=e^{-2t/\tau}(2S^{\rm inc})^{-1}\left[\sum_{l=1}^{\infty}A_l(e^{-2y_l^2 t}-1)\right], \tag{4.26}$$

where

$$S^{\rm inc}=1-\tfrac{1}{4}[(6\sqrt{2}l_T/x_0)\tanh(x_0/2\sqrt{2}l_T)+\operatorname{sech}^2(x_0/2\sqrt{2}l_T)],$$

where $y_l=(2l-1)(\pi\sqrt{2}l_T/x_0)(1/\tau)$, and A_l are given by (3.4) and (4.21).

In Eqs. (4.23)—(4.26) use has been made of an exact evaluation[30] of the summation $\sum_{l=1}^{\infty}A_l$ which is possible in the two extreme limits. The signal in the intermediate coherence domain is given by the conjunction of (3.4), (3.7)—(3.10), and (4.14) and (4.15). There is little advantage to rewriting the complete expressions, but the forms

$$\psi^{\eta_l}(t)=J_0((2l-1)\xi_{\rm coh}(t/\tau))e^{-\alpha t}+\int_0^t du\,\alpha e^{-\alpha(t-u)}J_0((2l-1)\xi_{\rm coh}(t^2-u^2)^{1/2}(1/\tau)), \tag{4.27}$$

$$\frac{1}{\tau}\tilde{\psi}^{\eta_l}\left[\frac{1}{\tau}\right]=\{[(1+\alpha\tau)^2+\xi_{\rm coh}^2(2l-1)^2]^{1/2}-\alpha\tau\}^{-1}, \tag{4.28}$$

that (4.14) and (4.15) take in the light of the continuum approximation (4.16) and of the definition (4.22) of the transport length may be helpful. The quantity $\xi_{\rm coh}$ introduced in (4.27), (4.28) and an analogous quantity $\xi_{\rm inc}$ to be used below are defined as

$$\xi_{\rm coh}=4\pi V\tau a/x_0=2\sqrt{2}\pi(l_T)_{\rm coh}/x_0\,, \tag{4.29}$$

$$\xi_{\rm inc}=2\pi\sqrt{F\tau}a/x_0=\sqrt{2}\pi(l_T)_{\rm inc}/x_0\,. \tag{4.30}$$

Note that $\xi_{\rm inc}$ is identical to the parameter a of Ref. 1.

Several experimentally relevant reasons, which make it desirable that observations of the *buildup* of the delayed fluorescence be made as well as those of its decay, have been discussed elsewhere.[1,6] When actual observations of the buildup are carried out, expressions (3.7) and (3.9) and the various particular cases including (4.23) and (4.25) may be used directly. However, in the plots below only the decay signals have been shown because they are numerically easier to obtain and contain all the physics of interest.

How could the experiments under discussion ascertain whether exciton motion is coherent, and, if so, measure the degree of coherence? We now address this practical question with the help of the above results. In Fig. 1 is plotted the time-dependent observable $-\Delta\Phi^d(t)$, which, as explained in Sec. III, is the difference of the (normalized) delayed fluorescence signals with and without rulings. The family of dashed lines represents completely incoherent motion and corresponds to (4.26). The family of solid lines represents purely coherent motion and corresponds to (4.24). There are corresponding pairs in the two families, a,b,c,d referring, respectively, to four different values of l_T/x_0, as shown. Although no dramatic effects such as oscillations are seen in the coherent curves of Fig. 1, their shapes are considerably different from those of the incoherent curves.

To show how clearly discernible the differences are, we present Fig. 2. Equation (4.24) shows that the coherent theory, if used to fit observations, would yield a value of $\xi_{\rm coh}$, which, from a knowledge of the ruling period and the lifetime, would give a value of the exciton velocity. On the other hand, use of the incoherent theory through (4.26) would yield a value of $\xi_{\rm inc}$ and thence the exciton diffusion constant. Given an experimental curve and two competing theories it is thus necessary on one hand to decide between the applicability of the two theories and on the other to determine the value of the appropriate parameter

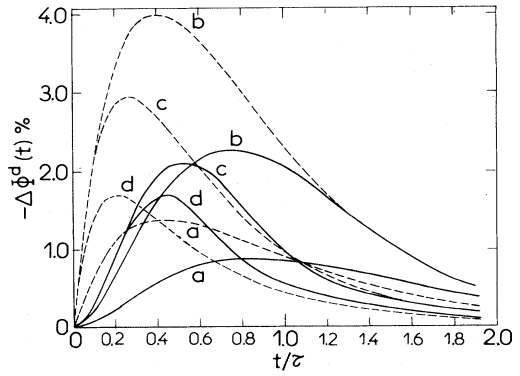

FIG. 1. Delayed fluorescence decay signal $-\Delta\Phi^d(t)$ plotted as a function of the dimensionless time t/τ for the extreme cases of pure coherence and complete incoherence. Curves a,b,c,d, refer, respectively, to the values 0.05,0.15,0.35,0.45 of l_T/x_0, the ratio of the transport length to the ruling period. Solid lines represent the purely coherent case, and the dashed lines the completely incoherent case. Curves of the latter kind have been already observed experimentally (e.g., Fig. 5 of Ref. 1).

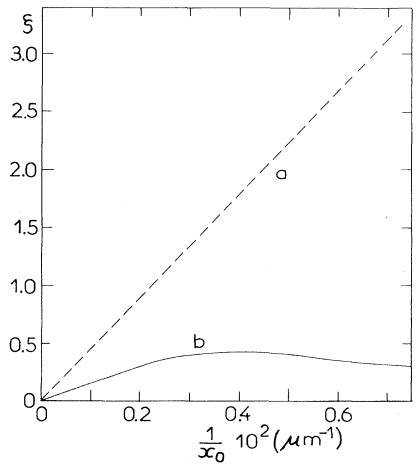

FIG. 2. Plot vs $(1/x_0)$, the spatial frequency of the rulings, of the dimensionless quantities $\xi_{\rm coh}=2\pi\sqrt{2}(l_T)_{\rm coh}/x_0$ for the purely coherent case (curve a) and $\xi_{\rm inc}=\pi\sqrt{2}(l_T)_{\rm inc}/x_0$ for the completely incoherent case (curve b), as obtained by graphically inverting expressions (4.24) and (4.26) in the text for the same "observed" signal $-\Delta\Phi^d(t)$. The latter is obtained by fitting curves such as those in Fig. 1. The straight-line behavior a indicates that the correct theory has been used to interpret the measurements. The clear departure of curve b from straight-line behavior shows that the theory used for b is incorrect. The straight line a corresponds to a transport length $l_T=50\ \mu$m.

(velocity or V versus diffusion constant or F). One way to achieve both these goals is to attempt best fits and decide which theory (and parameter value) describes the observations more closely. An experimentally preferable way, however, is as follows. One inverts the two theoretical expressions to give the two basic parameters $\xi_{\rm coh}$ and $\xi_{\rm inc}$ in terms of the observable. From the measured values of the observable, $\xi_{\rm coh}$ and $\xi_{\rm inc}$ are determined. These two sets of experimental values of ξ are then plotted versus the experimentally measured quantity $1/x_0$. A straight line passing through the origin, if obtained, indicates that the correct theory has been applied and the slope yields the value of velocity or diffusion constant. This procedure, which we have also explained[30] in the context of steady-state observables, possesses the advantage of using linearity, and departures from it, for deciding between the theories.

As an example we consider a system in which exciton motion is *coherent*. A measurement is made with a certain ruling period x_0. By varying (l_T/x_0), curves such as the dashed lines of Fig. 1 are used to produce a best fit to the observed plot. A value of $\xi_{\rm inc}$ is obtained from it. A new measurement with a different value of the ruling period is now made and a new value of $\xi_{\rm inc}$ is obtained similarly. The procedure is repeated for several values of x_0 and a plot of the "experimental" quantities $\xi_{\rm inc}$ and x_0 is made. This is curve b of Fig. 2. By using curves such as the solid lines of Fig. 1, an identical procedure yields curve a. Figure 2 clearly shows that, if exciton motion is purely coherent, the incoherent motion theory will be experimentally shown to be completely inadequate if the above procedure is followed. Needless to say, if the actual motion is incoherent, the coherent theory would show clear departure from linearity.

The results of the above procedure as reported in Fig. 2 do not make clear how bad the fits of the "incorrect" theory are to the individual time-dependent curves for each value of x_0. Since the more inadequate these fits are the clearer is the experimental procedure of distinguishing between the two, it is important to appreciate the extent of the inadequacy. To this end we present Fig. 3. A single x_0 is considered in the "measurement." The "experimental" values of $-\Delta\Phi^d(t)$ are multiplied by $e^{2t/\tau}$ to produce the function $E^d(t)$ of (3.10). A graphical inversion of the purely coherent and completely incoherent expressions which fit the "observed" curve best is carried out to produce "experimental" values of $\xi_{\rm coh}t/\tau$ and $\xi_{\rm inc}t/\tau$, respectively. Figure 4 shows the $E^d(t)$ curves. The single coherent curve which fits the "observed" curve completely (by assumption) is a. Curves b, c, d, and e are several possible fits in four different time regions, based on the incoherent $E^d(t)$ corresponding to (4.26). Visual inspection already shows the inadequacy of the incoherent curves. Figure 3, where the values of $\xi_{\rm coh}t/\tau$ and $\xi_{\rm inc}t/\tau$ as determined from Fig. 4 are plotted as functions of t/τ, makes the inapplicability of the incoherent theory transparent.

The above discussion has centered on the clear differences in the experimental manifestation of the *extreme* limits of exciton motion. The intermediate behavior is shown in Figs. 5 and 6. The quantity plotted is $-\Delta\Phi^d(t)$ as given by (3.10), (3.4), (4.27), and (4.28). In Fig. 5, the ratio l_T/x_0 of the transport length to the ruling period is held constant whereas in Fig. 6, the quantity held constant is the bandwidth for a given ruling period, or more generally, the ratio $\sqrt{2}V\tau a/x_0$ of the coherent transport length to the ruling period. If the transport length l_T is known from an independent measurement, a family of plots such as Fig. 5 may be used to determine the degree of coherence. For a given measured x_0 such a family of

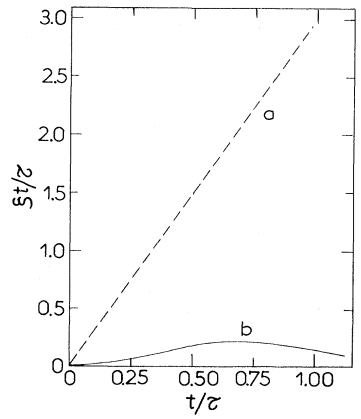

FIG. 3. Plot of the dimensionless quantities $\xi_{\rm coh}t/\tau$ for the purely coherent case (curve a) and $\xi_{\rm inc}t/\tau$ for the completely incoherent case (such as curve b) as obtained by graphically inverting expressions such as (3.10) in the text for the same "observed" $E^d(t)$ of Fig. 4. As in Fig. 2, the straight-line behavior a indicates that the (coherent) theory is correct and the clear departure of curve b from linearity that the (incoherent) theory is inapplicable. See text for further discussion. The line a corresponds to $\xi_{\rm coh}=3.0$.

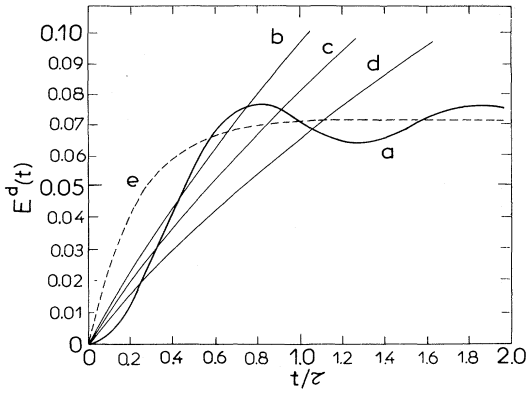

FIG. 4. Function $E^d(t)$ from (3.10) in the text, which is the decay signal $-\Delta\Phi^d(t)$ multiplied by $e^{2t/\tau}$ plotted as a function of t/τ. Curve a corresponds to the "observed," i.e., the purely coherent case, and curves b,c,d, to several possible fits to a on the basis of the incoherent theory in the $t<\tau$ region. It is clearly seen that the incoherent theory is inapplicable. The dashed line curve e is close to a in the region of large times ($t>\tau$).

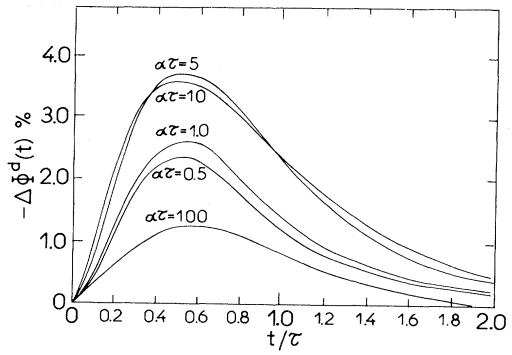

FIG. 6. Intermediate coherence behavior as reflected in $-\Delta\Phi^d(t)$ plotted as a function of t/τ with the exciton bandwidth held constant for a given ruling period, or more generally, with the ratio $V\tau a/x_0$ held constant (at the value 0.25). The usefulness of the plots is in deducing the degree of coherence experimentally if the bandwidth is known from an independent measurement.

plots is constructed (or x_0 is varied to give $l_T/x_0=0.2$, as in Fig. 5) and the value of $\alpha\tau$ is read off from the best fitting curve. Knowledge of l_T [see (4.22)] and $\alpha\tau$ then gives $V\tau$ and therefore the mean free path, or V/α or any desired combination thereof. Figure 6 is useful to the experimental determination of coherence in situations when the exciton velocity or bandwidth is known. The procedure is entirely similar to that for Fig. 5. Note that in Fig. 6 the ordering of the curves is not monotonic with $\alpha\tau$, in spite of the fact that l_T decreases montonically as the degree of incoherence (or $\alpha\tau$) is increased. This is due to the fact that, for the values chosen, l_T starts out at the coherent end being larger than the critical value (for a given value of x_0) for which the size of the motion effect is largest. As $\alpha\tau$ is varied, l_T passes through this critical value but then moves away from it resulting once again in a smaller effect. It is hoped that the above analysis will be helpful to future experiments along these lines.

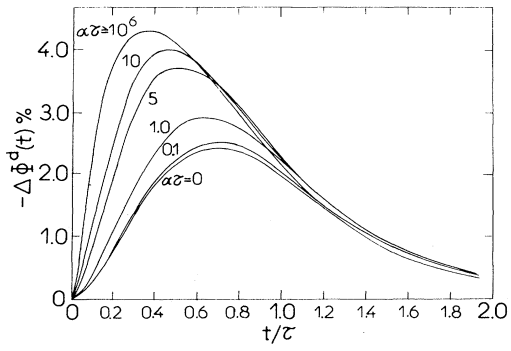

FIG. 5. Intermediate coherence behavior as reflected in the delayed fluorescence decay signal $-\Delta\Phi^d(t)$ plotted as a function of the dimensionless time t/τ. The value of l_T/x_0 is 0.2 for all curves. The practical usefulness of the plot is in ascertaining the degree of coherence experimentally if l_T (e.g., the diffusion length) is known from an independent measurement. The lowermost curve $\alpha\tau=0$ is the coherent case, while the uppermost one $\alpha\tau=10^6$ is already indistinguishable from the completely incoherent case.

V. VALIDITY OF THE ASSUMPTIONS UNDERLYING THE THEORY

The primary assumptions underlying the discussion, expressions, and plots of Sec. IV above are (a) the one-dimensional nature of the crystal, (b) the nearest-neighbor nature of the transfer interactions V, (c) the applicability of the bilinear annihilation term in (2.1), (d) the applicability of generalized master equations for describing exciton transport in Ronchi ruling experiments, and (e) the applicability of the particular intermediate memory functions $W_{mn}(t)$ of (4.6). The validity of these assumptions will now be discussed in turn.

Assumptions (a) and (b) are not present in the analysis of Secs. II and III. They have been made only in Sec. IV and only for simplicity. That the rulings provide a one-dimensional spatial inhomogeneity is one of the physical reasons for assumption (a). In a crystal which is not one-dimensional, the quantities V, α, a, F, etc., are to be taken as effectively one dimensional. In any case assumption (a) may be relaxed quite easily.[31] The same is true of (b). There is also a sound physical reason for the latter assumption: Triplet excitons are known to have very short-ranged transfer matrix elements since the responsible mechanism is that of exchange interactions.

Some recent theoretical work[11] on exciton annihilation has cast doubt on the validity of the bilinear annihilation term $-\gamma' P_m^2(t)$ in (2.1). It has been found that generally that term should be replaced by one which is nonlocal both in time and in space.[32] It has been argued that, under certain conditions, for exciton motion which is sufficiently fast, the term may be taken to be local in time, and that it is quite likely that these conditions are satisfied in most systems of interest.[11] However, the nonlocal nature in space persists. The traditional usage of the local term of

(2.1) has been reconciled with the fact that its consequences are identical to those of the nonlocal term provided the exciton distribution is initially homogeneous in space. While most traditional usage has indeed been in the context of homogeneous initial distributions, conflict would be expected for inhomogeneous initial distributions such as those in Ronchi ruling experiments. However, the conflict disappears in the deductions used in this paper for the following reasons. The nonlocal term is $\sum_n \Lambda_{m-n}P_n^2(t)$, the relation to the local term $-\gamma' P_m^2(t)$ being

$$\sum_m \Lambda_m = \gamma' \ . \tag{5.1}$$

There is little doubt that the two terms would generally predict different behavior for P_m. However, the delayed fluorescence signal is collected from the entire crystal and thus involves a summation of the term over all m. And one has

$$\sum_m \sum_n \Lambda_{m-n}P_n^2 = \sum_m \left[\sum_n \Lambda_n \right] P_m^2 = \sum_m \gamma' P_m^2 \tag{5.2}$$

as a result of the translational periodicity of the crystal. Thus, although in the light of the theory of Ref. 11, $(dP_m/dt)_{\text{annihilation}}$ is given incorrectly by the local annihilation term in (2.1), the summed quantity $\sum_m (dP_m/dt)_{\text{annihilation}}$ is always given correctly by its use. And it is the summed quantity that appears in the delayed fluorescence signal obtained in the Ronchi ruling experiments. The use of the local term for the present analysis is therefore quite valid.

Assumption (d) concerns the applicability of the GME itself. In the specific context of Ronchi ruling experiments there are three classes of initial conditions under which the GME applies without approximation. The first is when each exciton is initially completely site localized, the initial probability distribution being due to the exciton *number* varying in space. For each exciton, the GME is then valid exactly because the density matrix $\rho(0)$ is initially diagonal. The effect due to the various excitons is additive. This situation is that encountered in the diffusion equation analyses.[1-6] More general initial conditions are, however, possible in these experiments. A single exciton may be spread throughout the crystal. The second class of initial conditions under which the GME is exact for Ronchi ruling experiments is one in which an individual exciton is in a single Bloch state[8(b),9] or in a thermalized equilibrium state.[9] In the third class the excitons may be spread out to an intermediate degree (neither fully localized nor fully delocalized) but in such a way that the *ensemble average* of the off-diagonal elements of $\rho(0)$ in the site representation vanishes. This last class has the first two as special cases, generally involves a *mixed* initial density matrix,[33] and provides the practical justification for the use of (2.1). It is clearly possible to construct special initial conditions for which (2.1) is not valid.[34] However, in such cases, one can always redo the analysis by augmenting the GME (2.1) through a driving term arising from the initial off-diagonal $\rho(0)$. This procedure has been explained in detail in Refs. 8 and 9.

Finally we discuss the applicability of the particular intermediate memory functions (4.6) used in Sec. IV. The physics underlying them is that of the equation

$$\frac{\partial \rho_{mn}}{\partial t} = -iV(\rho_{m+1n}+\rho_{m-1n}-\rho_{mn+1}-\rho_{mn-1}) - \alpha(1-\delta_{mn})\rho_{mn} \ , \tag{5.3}$$

where ρ is the exciton density matrix. Equation (5.3) is the simplest transport equation containing the essential features of motion with arbitrary degree of coherence.[35] For $\alpha \to 0$, i.e., in the absence of scattering, it clearly reduces to the von Neumann equation in complete equivalence to the Schrödinger equation (4.3). It can be shown[9] that in the opposite limit ($\alpha \to \infty, V \to \infty$, $V^2/\alpha = \text{const}$), it becomes the simple master (hopping) equation (4.1) with hopping rates $F = 2V^2/\alpha$. We have used (5.3) in the illustrative calculations of Sec. IV precisely because of its simplicity. The bandwidth associated with it is[36] $4V$, the average group velocity is $\sqrt{2}Va$, the mean free path is $\sqrt{2}Va/\alpha$, and the diffusion constant for small V/α is $2V^2a^2/\alpha$. Much physics can thus be described in terms of the small number of parameters in it. For these reasons it has been used in several recent investigations of the effect of transport coherence on sensitized luminescence,[10] annihilation,[11] and singlet gratings.[12] If necessary, the equation may be replaced by more detailed transport descriptions. An example might be that of the stochastic Liouville equation (SLE), written in the simplified form[9,37]

$$\frac{\partial \rho_{mn}}{\partial t} = -iV(\rho_{m+1n}+\rho_{m-1n}-\rho_{mn+1}-\rho_{mn-1}) - \alpha(1-\delta_{m,n})\rho_{mn} + \delta_{mn}\gamma_1(\rho_{m+1m+1}+\rho_{m-1m-1}-2\rho_{mm}) \ . \tag{5.4}$$

The SLE (5.4) reduces to (5.3) when $\gamma_1 = 0$, but describes "phonon-assisted" motion[38] through the rates γ_1 in addition to the "phonon-hindered" motion described by (5.3) through V and α. The propagator $\tilde{\psi}^{\eta_l}$ corresponding to (5.4) is obtained in the Laplace domain[9] as

$$\tilde{\psi}^{\eta_l}(\epsilon) = \{[(\epsilon+\alpha)^2 + 16V^2\sin^2(\eta_l/2)]^{1/2} - \alpha + 4\gamma_1\sin^2(\eta_l/2)\}^{-1} \ . \tag{5.5}$$

Substitution in (3.7)–(3.10) and calculation of the resulting delayed fluorescence signals are straightforward, although tedious numerical integrations are required. These integrations have been carried out in other contexts[39] and the *steady-state* Ronchi ruling signals have also been obtained explicitly.[30] The general expressions for the delayed fluorescence given in Sec. III above, in particular (3.7)–(3.10), can be used easily in conjunction with transport instruments which are even more detailed than (5.3) or (5.4) if such detail is warranted by the particular experimental situation. Multiple scattering times,[26] several channels of motion,[23-25] specific inclusion of temperature effects,[24] and memory functions corresponding to observed optical spectra[7] are some of the features that could thus be included, if required, in the general analysis of Secs. II and III.

VI. DISCUSSION

A general theory of coherence effects in exciton transport as might be seen via delayed fluorescence in Ronchi ruling experiments and a practical prescription for the experimentalist to ascertain those effects from measurements have been the two goals of the present investigation. The point of departure is the GME (2.1), the exact solutions for the exciton probabilities are (2.12), (2.13), and (2.15), and general results for the delayed fluorescence signals are (3.7)—(3.10). Signals for completely incoherent motion have been recovered in (4.25) and (4.26), new results for purely coherent motion are in (4.23) and (4.24), and intermediate results valid for arbitrary degree of coherence are obtained from (4.27) and (4.28). These various signals have been plotted in Figs. 1, 5, and 6: the extremes of coherence and incoherence in Fig. 1, and the intermediate cases in Figs. 5 and 6. The practical prescription for an experimental determination of whether exciton motion is coherent and incoherent and for the measurement of the degree of coherence has been given in the discussion relevant to the plots.

There are two principal ways in which the differences between coherent and incoherent motion could be manifested in time-dependent delayed fluorescence decay signals: oscillations and the shape (concave versus convex) near the origin. Oscillations can occur only for coherent behavior, are an unambiguous consequence of wavelike motion, and can be appreciated clearly in Fig. 7 which is a plot of the function $E^d(t)$ of (3.10). However, the experimental observable is $-\Delta\Phi^d(t)$ which is the result of multiplying $E^d(t)$ by $e^{-2t/\tau}$. Unless the signal-to-noise ratio is improved considerably, clear observations of oscillations are unlikely because oscillations appear further on on the time scale where the value of $-\Delta\Phi^d(t)$ is small. On the other hand, distinction on the basis of the difference in shapes for $t < \tau$, which is also clearly seen in Figs. 4 and 7, is indeed possible practically. It is of interest to note that, apart from the l summation arising from the square-wave (rather than pure sinusoidal) nature of the initial inhomogeneity, the function $E^d(t)$ is, in essence, the square of the exciton propagator (Fourier transformed) subtracted from 1.

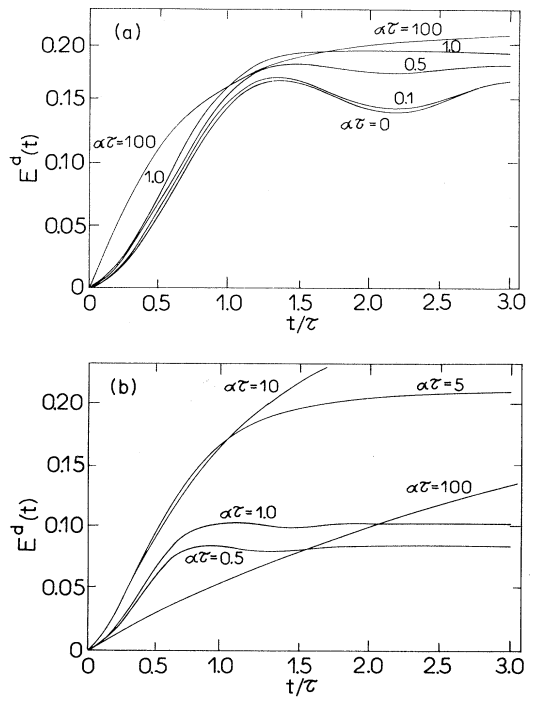

FIG. 7. Function $E^d(t)$ of (3.10) in the text, plotted as a function of t/τ to show the entire intermediate behavior with arbitrary degree of coherence. In (a) the ratio l_T/x_0 is held constant (at the value 0.2) and in (b) the ratio $V\tau a/x_0$ is held constant (at the value 0.25).

As mentioned in Sec. I, there are four characteristic lengths in the system under consideration: (i) the lattice constant a, i.e., the distance between two crystal sites, which is of the order of 5—10 Å, (ii) the mean free path, i.e., the average distance the exciton travels between two scattering events, which could be of the order of a lattice constant (or formally even less) in the case of highly diffusive or hopping motion, or many hundreds of lattice constants in the case of highly wavelike or coherent motion, (iii) the "transport length" l_T which is the average distance covered by the exciton during its lifetime, which reduces to the diffusion length l_D in the case of motion which is diffusive at times of the order of a lifetime, and which could be of the order of microns, and (iv) the ruling period x_0 which is the quantity that can be manipulated in the experiments.

For the purposes of the experiment, the lattice constant a hardly enters into the discussion. Furthermore, for completely diffusive motion, the mean free path is of little interest. In such a case one varies x_0 to determine l_T which may be called l_D since the motion is diffusive by assumption. Independent knowledge of the lifetime τ then allows one to deduce the diffusion constant D from l_D. However, if the motion is completely coherent, the measured transport length l_T is *not* the distance covered by an exciton random walker during the lifetime. Instead, it is the distance covered by a coherent exciton moving without scattering during its lifetime. What would be deduced from l_T and the lifetime is then not the exciton diffusion constant (which is proportional to the square of l_D or l_T) but the exciton *velocity* (which is proportional to l_T itself). If the motion possesses an intermediate degree of coherence, the mean free path becomes important since it then neither equals, or is smaller than, a (extreme incoherence) nor is it infinite or at least much larger than l_T (extreme coherence). To measure this mean free path is to measure the degree of coherence in the system. The Ronchi ruling experiment can carry out such a measurement, at least in principle, by varying the ruling period. Coherence effects would be particularly apparent when the ruling period x_0 is of the order of the mean free path.

It is also possible to discuss the above in terms of the four characteristic times that exist in the experiments: (i) the time the exciton takes to traverse, in a wavelike fashion, i.e., in the absence of scattering, the distance between two sites, which is proportional to the reciprocal of the exciton bandwidth and thus to $1/V$, (ii) the time between successive scattering events, which is $1/\alpha$, (iii) the lifetime τ, and (iv) the time the exciton takes to traverse

the ruling period x_0, which will be called τ_R. The ratio of the first two, i.e., of $1/V$ and $1/\alpha$, is generally used to describe the degree of coherence. Thus, if scattering occurs within a time of the order of $1/V$, the motion is totally incoherent. The measured quantity is τ_R. If, by varying the ruling period x_0, τ_R is changed as to be of the order of $1/\alpha$, coherent effects will be manifested in the measurements.

The analysis in the present paper is applicable to *any* spatially periodic excitation and is not restricted to Ronchi rulings. One merely changes the g^k in (2.8) to have the appropriate form. For instance, an initial sinusoidal inhomogeneity obtained with the use of two interfering laser beams in some delayed fluorescence observations[5] as well as in recent work on singlet motion[40,41] and on energy transfer in inorganic solids,[42,43] can be represented by

$$g^k = \tfrac{1}{2}[\delta_{k,0} + \tfrac{1}{2}(\delta_{k,\eta} + \delta_{k,-\eta})] .$$

The various comments made in the GME analysis[9,12] of such a situation, concerning the directness and conceptual simplicity of the observations, apply equally well to the experimental approach[1-6] discussed in the present paper.

ACKNOWLEDGMENTS

One of us (V.M.K.) acknowledges partial support of this research by the National Science Foundation Grant No. DMR-81-11434.

*Permanent address: Department of Physics and Astronomy, University of Rochester, Rochester, New York 14627.

[1]V. Ern, P. Avakian, and R. E. Merrifield, Phys. Rev. 148, 862 (1966).

[2]V. Ern, Phys. Rev. Lett. 22, 343 (1969).

[3]P. Avakian and R. E. Merrifield, Phys. Rev. Lett. 13, 541 (1964).

[4]S. Arnold, J. L. Fave, and M. Schott, Chem. Phys. Lett. 28, 412 (1974); J. B. Aladekomo, S. Arnold, and M. Pope, Phys. Status Solidi B 80, 333 (1977); V. Ern, J. Chem. Phys. 56, 6259 (1972); A. Fort and V. Ern, Chem. Phys. Lett. 74, 519 (1980).

[5]B. Nickel, Ber. Bunsenges. Phys. Chem. 76, 582 (1972).

[6]V. Ern and M. Schott, in *Localization and Delocalization in Quantum Chemistry,* edited by O. Chalvet (Reidel, Dordrecht, 1976), Vol. II, p. 249, a review.

[7]V. M. Kenkre and R. S. Knox, Phys. Rev. B 9, 5279 (1974); V. M. Kenkre, J. Stat. Phys. 30, 313 (1983).

[8](a) V. M. Kenkre, in *Statistical Mechanics and Statistical Methods in Theory and Application,* edited by U. Landman (Plenum, New York, 1977); (b) J. Stat. Phys. 19, 333 (1978).

[9]V. M. Kenkre, in *Exciton Dynamics in Molecular Crystals and Aggregates,* edited by G. Höhler (Springer, Berlin, 1982).

[10]V. M. Kenkre and Y. M. Wong, Phys. Rev. B 23, 3748 (1981); V. M. Kenkre and P. E. Parris, *ibid.* 27, 3221 (1983).

[11]V. M. Kenkre, Phys. Rev. B 22, 2089 (1980); Z. Phys. B 43, 221 (1981).

[12]V. M. Kenkre, Phys. Rev. B 18, 4064 (1978); Phys. Lett. 82A, 100 (1981); Y. M. Wong and V. M. Kenkre, Phys. Rev. B 22, 3072 (1980).

[13]M. Pope and C. E. Swenberg, *Electronic Processes in Organic Crystals* (Oxford University, New York, 1982), and references therein.

[14]D. C. Hoesterey and G. W. Robinson, J. Chem. Phys. 54, 1369 (1971), and references therein.

[15]D. Haarer, D. Schmid, and H. C. Wolf, Phys. Status Solidi 23, 633 (1967); D. Haarer and H. C. Wolf, Mol. Cryst. Liq. Cryst. 10, 359 (1970); H. Kolb and H. C. Wolf, Z. Naturforsch Teil A 27, 51 (1972); R. Schmidberger and H. C. Wolf, Chem. Phys. Lett. 32, 18 (1975), and references therein.

[16]J. Rosenthal, L. Yarmus, N. F. Berk, and W. Bizzaro, Chem. Phys. Lett. 56, 214 (1978).

[17]H. C. Brenner, in *Triplet State ODMR Spectroscopy,* edited by R. H. Clarke (Wiley, New York, 1982), p. 185.

[18]C. B. Harris and D. A. Zwemer, Ann. Rev. Phys. Chem. 29, 473 (1978).

[19]D. M. Burland and A. H. Zewail, Adv. Phys. Chem. 50, 385 (1980); D. D. Smith and A. H. Zewail, J. Chem. Phys. 71, 3533 (1979).

[20]A. H. Francis and R. Kopelman, in *Excitation Dynamics in Molecular Solids,* Vol. 49 of *Topics in Applied Physics,* edited by W. M. Yen and P. M. Selzer (Springer, Berlin, 1981), p. 214.

[21]R. D. Wieting, M. D. Fayer, and D. D. Dlott, J. Chem. Phys. 69, 1996 (1978); D. D. Dlott, M. D. Fayer, and R. D. Wieting, *ibid.* 69, 2752 (1978).

[22]A. J. van Strien and J. Schmidt, Chem. Phys. Lett. 86, 203 (1982); A. J. van Strien, J. Schmidt, and R. Silbey, Mol. Phys. 46, 151 (1982); A. J. van Strien and J. Schmidt, in Physics and Chemistry of Molecular Structures, edited by I. Zschokke-Gränacher (Reidel, Dordrecht, in press).

[23]H. Haken and G. Strobl, in *The Triplet State,* edited by A. B. Zahlan (Cambridge University, Cambridge, 1967).

[24]R. Silbey, Ann. Rev. Phys. Chem. 27, 203 (1976).

[25]P. Reineker, in *Exciton Dynamics in Molecular Crystals and Aggregates,* edited by G. Höhler (Springer, Berlin, 1982).

[26]V. M. Kenkre, Phys. Rev. B 11, 3406 (1975); 12, 2150 (1975); Phys. Lett. 65A, 391 (1978).

[27]The ratio of this reduced bandwidth to the scattering rate is, in effect, the ratio of the mean free path of the exciton to the period of the Ronchi ruling.

[28]The coefficient S_l given by (2.9) is just the Fourier amplitude of the lth spatial harmonic for the simplest Ronchi ruling having equal size open and opaque strips. For the more general ruling geometry for which the open strip is a fraction $r<0.5$ of the ruling period x_0 one has $S_l=-(1/r\pi l)\sin(\pi l r)$. As also shown in Refs. 1 and 6, if one considers some amount of stray light Δi present in the shadow regions, the coefficients S_l given above are diminished by the factor $\sigma_r'=(1-\Delta i/ri_0)$. It should be noted that in the above expression for S_l, l takes on all integer values, even as well as odd.

[29]S. M. Phatak and V. M. Kenkre (unpublished).

[30]V. M. Kenkre, A. Fort, and V. Ern, Chem. Phys. Lett. 96, 658 (1983).

[31]Work along this direction, as well as the analysis of crystals containing several molecules per unit cell, is in progress.

[32]As explained in Refs. 9 and 11, the nonlocal nature of the term has nothing to do with coherence effects and appears even for completely incoherent motion.

[33]See, e.g., L. D. Landau and E. M. Lifschitz, in *Statistical Physics* (Pergamon, London, 1958).

[34]An interesting illustration of initial conditions wherein the

GME may not be used in the form of (2.1) is provided by the amplitude distribution $C_m(0)=\text{const}\cos(\eta m/2)$. It corresponds to populating two exciton k states with equal and opposite quasimomenta, $\eta/2$ and $-\eta/2$, respectively, and to an initial probability distribution $P_m(0)=\text{const}[1+\cos(\eta m)]$. If the latter form of $P_m(0)$ is used with (2.1), one would conclude that the exciton distribution evolves in time essentially as explained in Sec. IV. However, if the above $C_m(0)$ is substituted in the Schrödinger equation (4.3), one concludes that $P_m(t)=P_m(0)$ for all time. The reason for the contradiction is that, in this particular example, the initial driving term which is dropped in the form (2.1) of the GME, makes a contribution to the evolution of $P_m(t)$ which is exactly equal and *opposite* to that made by (2.1). In a realistic situation the above amplitudes $C_m(0)$ are expected to have phase factors which vary slightly but randomly from ensemble member to ensemble member with the result that, while $\rho_{mn}(0)$ has a zero ensemble average, $\rho_{mn}(0)=P_m(0)$ is still given by $\text{const}[1+\cos(\eta m)]$. The initial condition then belongs to what has been called the third class in the text and the GME (2.1) is again valid.

[35]P. Avakian, V. Ern, R. E. Merrifield, and A. Suna, Phys. Rev. 165, 974 (1968).

[36]Here, and everywhere in the present paper, we have put $\hbar=1$ for simplicity.

[37]R. P. Hemenger, K. Lakatos-Lindenberg, and R. M. Pearlstein, J. Chem. Phys. 60, 3271 (1974).

[38]The terms "phonon assisted" and "phonon hindered" refer to microscopic derivations of the SLE such as that in Ref. 24, although the terms may arise from general sources as in Refs. 23 and 25.

[39]D. W. Brown and V. M. Kenkre (unpublished).

[40]J. R. Salcedo, A. E. Siegman, D. D. Dlott, and M. D. Fayer, Phys. Rev. Lett. 41, 131 (1978).

[41]K. A. Nelson, R. Casalegno, R. J. Dwayne Miller, and M. D. Fayer, J. Chem. Phys. 77, 1144 (1982).

[42]P. F. Liao, L. M. Humphrey, D. M. Bloom, and S. Geschwind, Phys. Rev. B 20, 4145 (1979).

[43]C. M. Lawson, R. C. Powell, and W. K. Zwicker, Phys. Rev. Lett. 46, 1020 (1981).